ACI STRUCTURAL JOURNAL TECHNICAL PAPER

Title no. 91-S11

Confinement of High-Strength Concrete Columns

by Shamim A. Sheikh, Dharmendra V. Shah, and Shafik S. Khoury

High-strength concrete (HSC) with compressive strength of 8000 psi (55 MPa) or higher is commonly used in columns at present. However, very little is known about its behavior under large inelastic deformations, particularly when subjected to severe earthquakes, and most building codes do not provide the required design guidelines. Results from four high-strength concrete specimens, three nonprismatic and one prismatic, tested under constant axial load and cyclic lateral loads simulating earthquake forces are presented here and compared with similar specimens of normal strength concrete (NSC). Concrete strength varied between 4500 and 8500 psi (31 and 59 MPa). Relevant provisions of the ACI Building Code are evaluated in light of the test data. Increase in the lateral steel contents resulted in an almost proportional increase in ductility and energy-absorption capacity of confined high-strength concrete, just as in the case of normal strength concrete. The required amount of confining steel appears to be proportional to the strength of concrete for a certain column performance if the axial load is measured in terms of P_o *rather than as a fraction of* $f'_c A_g$. *Useable compressive strain in the range of 0.01 to 0.02, and curvature ductility factors as high as 16, were observed in confined high-strength concrete columns.*

Keywords: axial loads; **columns (supports); confined concrete;** ductility; earthquakes; energy; **high-strength concretes;** hinges (structural).

Due to economic considerations, concrete strength in structures such as buildings, bridges, and offshore platforms has increased steadily during the last two decades. Concrete with compressive strength of 7000 to 9000 psi (48.3 to 62.1 MPa) was first used in areas with little or no seismic risk. However, in recent years, concrete with strength as high as 16,500 psi (113.8 MPa) has been used in buildings in seismic areas of the U.S. West Coast.[1] Growing interest in high-strength concrete (HSC) has caused most building codes to fall behind prevailing practice.

It is generally known that unconfined HSC displays more brittle behavior than normal strength concrete (NSC). For use in earthquake-resistant structures and to take advantage of economic savings through moment redistribution, it is imperative that various structural components behave in a ductile manner. Depending on the state of stress at a particular section, the concrete may also be required to display large ductility and energy-absorption capacity. Lateral reinforcement in the form of hoops or spirals is commonly used to confine concrete to achieve the required deformability. Results from several experimental studies have been reported in the literature[2-4] dealing with confined HSC members subjected to pure axial load or pure bending. Data from tests on specimens under combined flexure and axial load, however, are very limited,[5] particularly under high levels of axial load. Although dissipation of seismic energy through inelastic behavior of flexural members is preferable, hinging of columns during a severe earthquake may be unavoidable in many cases. Appropriate confinement of critical regions in columns is therefore needed to prevent brittle structural failure.

RESEARCH SIGNIFICANCE

Most of the design requirements for building codes such as ACI 318-89[6] have been developed over the years based on test results from normal strength concrete specimens. Data from realistically sized HSC specimens tested under realistic conditions are needed to check the validity of these requirements and, if necessary, to develop new guidelines. This paper presents test results from 8000 psi (55.2 MPa) concrete specimens confined by rectilinear ties. A comparison with similar NSC specimens is made and the code requirements for confining steel are evaluated against the performance of the specimens. The overall aim of this ongoing research is to develop a rational procedure and guidelines for the design of confining steel to achieve a certain structural performance.

TEST PROGRAM

Results from four large-scale columns tested under axial load and cyclic flexure are presented. Concrete with target compressive strength f_c' of 8000 psi (55.2 MPa) was used in the columns. These results are compared with those from earlier tests[7] on similar specimens made from normal strength concrete with nominal f_c' of 4000 psi (27.6 MPa). Since confining steel most affects the behavior of columns when the failure mode is dominated by compression failure of concrete, large axial loads were used in these specimens. Because most design codes allow high axial loads, and since during a se-

ACI Structural Journal, V. 91, No. 1, January-February 1994.
Received Sept. 2, 1992, and reviewed under Institute publication policies. Pertinent disucssion will be published in the November-December 1994 *ACI Structural Journal* if received by July 1, 1994.

Shamim A. Sheikh is a profesor of civil engineering at the University of Toronto. He is a member of joint ACI-ASCE Committees 441, Reinforced Concrete Columns; and 442, Response of Concrete Buildings to Lateral Forces. His research interests include confinement of concrete, earthquake resistance of reinforced concrete, and expansive cement and its application in deep foundation.

Dharmendra V. Shah received his initial degree in civil engineering from M. S. University, Baroda, India, in 1987. He received his MS in civil engineering from the University of Houston in 1991, and is working as a consulting engineer in Houston.

Shafik S. Khoury is an assistant professor in the Department of Structural Engineering at Alexandria University, Alexandria, Egypt. He received his PhD from the University of Houston in 1991. His research activities include concrete materials and reinforced concrete columns.

vere earthquake, the columns may be subjected to ultimate conditions, tests under axial loads in the range of code-allowed limits are needed to evaluate column behavior. Most of the relevant tests reported in the literature[5,8] deal with columns subjected to loads smaller than balanced loads. Particularly for high-strength concrete columns, there are limited test data available under high axial loads and cyclic flexure.

Specimens

Two types of specimens were used in this study. One specimen was a prismatic column 12 x 12 x 96 in. (305 x 305 x 2438 mm) with core dimensions of 10.5 in. (267 mm) square measured from center to center of the perimeter ties. Three nonprismatic specimens consisted of a 12 x 12 x 58-in. (305 x 305 x 1475-mm) column and a 20 x 30 x 32-in. (508 x 763 x 813-mm) stub at one end (see Fig. 1). The column core dimensions in this type of specimen were the same as in the prismatic specimen. All the columns contained eight No.6 longitudinal bars uniformly distributed around the core perimeter. Four corner bars were supported by bends in perimeter ties and internal diamond ties provided support to the middle bars. The ends of all the ties were hooked inside the core. Fig. 1 shows the section details and Table 1 contains the details of all the specimens. The stub specimens were cast in one batch and the prismatic specimen was cast in a separate batch. All the specimens were cast horizontally.

The first letter in the specimen designation refers to the steel configuration and is consistent with the designations used in an earlier test program.[9] The letter "S," if used, refers to the presence of stub followed by the sequence number of the specimen within the group of specimens in a test program. The last letter "H" refers to high-strength concrete.

Concrete

The target compressive strength for the ready-mix concrete was 8000 psi (55.2 MPa) in all the specimens. About 30 standard cylinders were cast with each pour and tested frequently to monitor concrete strength with age. Concrete strength f_c' for each specimen was obtained from the strength-versus-age

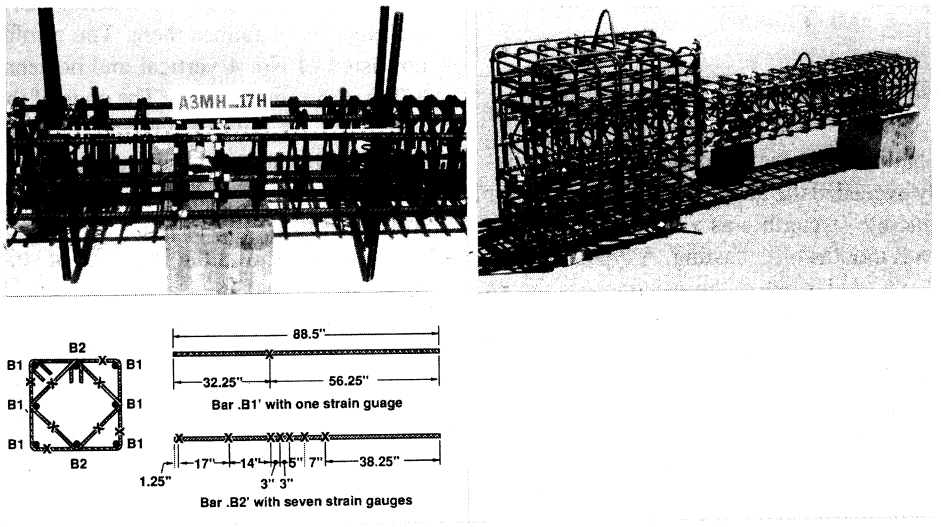

Fig. 1—Steel cages and instrumentation details

Table 1 — Specimen details and test results

Specimen	f_c', ksi	Lateral steel: Size @ spacing, in.	Lateral steel: ρ_s, percent	Lateral steel: f_{yh}, (ksi)	Lateral steel: $\frac{A_{sh}}{A_{sh}(ACI)}$	Axial load: $\frac{P}{f_c'Ag}$	Axial load: $\frac{P}{P_o}$	Moment, (k-in.): M_{smax}	Moment, (k-in.): M_{max}	Moment, (k-in.): M_i	Ductility factor: μ_Δ 0.8 P_{max}	Ductility factor: μ_ϕ 0.8 M_{max}	Ductility factor: μ_ϕ 0.9 M_{max}	Ductility ratios: $N_{\Delta 80}$	Ductility ratios: $N_{\Delta t}$	Ductility ratios: $N_{\phi 80}$	Ductility ratios: $N_{\phi t}$	Energy indicators: W_{80}	Energy indicators: W_t	Energy indicators: E_{80}	Energy indicators: E_t
AS-3H	7.85	#3@4.25	1.68	73.6	0.88	0.62	0.59	2238	2100	1753	3.2	10.5	9.0	12	15	31	35	29	44	178	204
AS-18H	7.93	#4@4.25	3.06	67.3	1.44	0.64	0.61	2381	2239	1716	3.9	14.0	11.0	19	23	43	59	53	54	384	458
AS-20H	7.78	#4@3.00	4.30	67.3	2.10	0.64	0.61	2637	2502	1678	5.4	16.5	13.5	25	52	80	98	83	213	935	1170
A-17H	8.57	#3@4.25	1.68	73.6	0.80	0.65	0.62	—	2311	1778	2.0	5.0	2.6	9	10	11	16	—	—	36	37
AS-3	4.81	#3@4.25	1.68	73.6	1.43	0.60	0.50	1806	1707	1371	4.7	19.0+	19.0+	23	32	63	74	84	127	610	753
AS-17	4.54	#3@4.25	1.68	73.6	1.52	0.77	0.63	1728	1594	1111	3.8	12.0	10.5	24	30	52	58	58	76	402	443
AS-18	4.75	#4@4.25	3.06	67.3	2.41	0.77	0.63	1892	1805	1112	6.7	17.5	14.5	44	53	80	92	263	290	897	1156

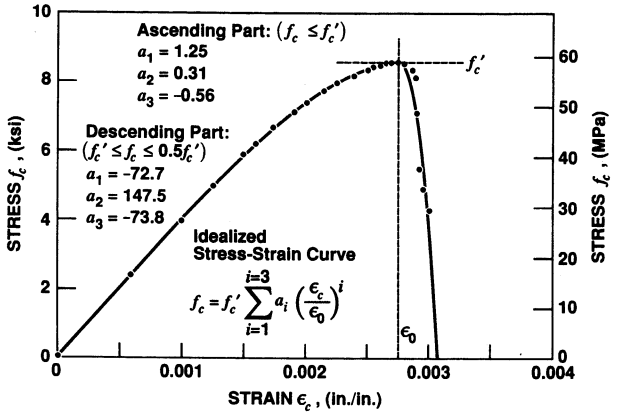

Fig. 2—Stress-strain curve of high-strength concrete

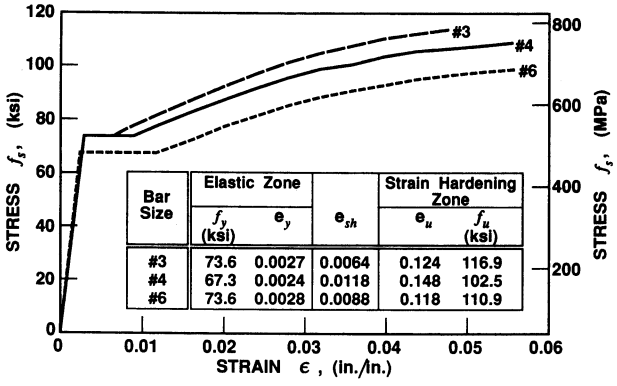

Bar Size	Elastic Zone f_y (ksi)	Elastic Zone e_y	e_{sh}	Strain Hardening Zone e_u	Strain Hardening Zone f_u (ksi)
#3	73.6	0.0027	0.0064	0.124	116.9
#4	67.3	0.0024	0.0118	0.148	102.5
#6	73.6	0.0028	0.0088	0.118	110.9

Fig. 3—Stress-strain curves of steel

relationship thus obtained. For the prismatic specimen, concrete strength easily exceeded the target strength, whereas for stub specimens concrete strength was a little less than the target strength even 3 months after casting. A typical stress-strain curve of concrete used in one of the specimens is shown in Fig. 2, which also includes an equation for the curve. The nominal maximum size of the crushed limestone was ½ in. (13 mm).

Steel

Deformed No. 3, 4, and 6 Grade 60 bars were used in the specimens. Longitudinal steel consisted of eight No. 6 bars in each specimen, providing steel content of 2.44 percent of the gross cross-sectional area of the column. Ties were made of No. 3 and 4 steel bars. Fig. 3 shows the stress-strain curves of steel up to about 5 percent strain. Rupture of the bars took place at strain values of about 12 to 14 percent. Each curve in the figure represents a minimum of three tests.

Cages

The length of the prismatic specimen cage was 94.5 in. (2.40 m). The ties were placed at specified spacing only in the test region, which was the middle 36-in. (914-mm) length of the specimen. Ties were placed at about three-fourths of the specified spacing outside the test region to avoid failure there. Two high-strength all-threaded 1⅛-in.- (28.6-mm)-diameter bars were placed symmetrically at 18 in. (457 mm) from the midspan on each side and kept vertical during

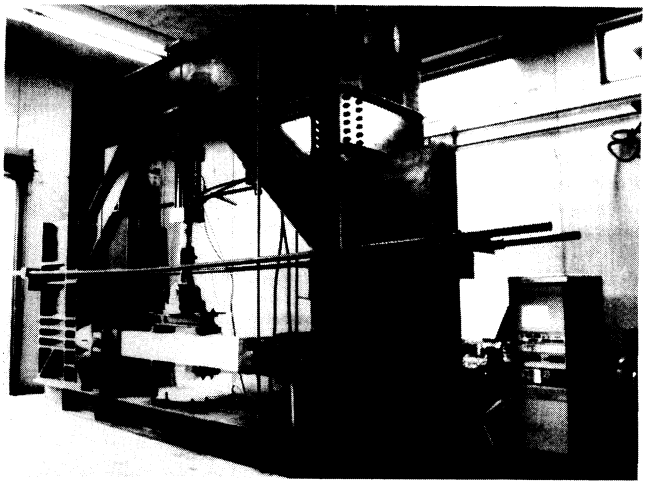

Fig. 4—Test frame with prismatic specimen in-place

casting. These bars were used to apply the upward lateral loading (Fig. 1).

The reinforcing cage for each stub specimen consisted of two parts, one for the column and the other for the stub (Fig. 1). The column longitudinal bars extended through the stub to ¾ in. (19 mm) from the end in all the specimens. The ties were placed at specified spacing within the column test region, approximately 36 in. (914 mm) adjacent to the stub. Outside the test region, tie spacing was reduced to minimize the chances of failure there. The reinforcement in the stub consisted of No. 4 vertical and horizontal stirrups at about 3.0-in. (76-mm) spacing. The ends of the ties were anchored inside the core with extension lengths conforming to ACI 318-89.[6] No anchorage failure was observed in any specimen.

Instrumentation

Fig. 1 also shows the locations of strain gages on longitudinal and lateral steel in stub specimens. Two sets of ties closest to the stub were instrumented with strain gages. A total of 36 gages was used in each stub specimen. In the prismatic specimen, a set of ties at midspan was instrumented with eight strain gages in the same manner as the one shown in Fig. 1. Another set of ties about 24 in. (612 mm) away was instrumented with two strain gages. Six longitudinal bars in this specimen were gaged at midspan and two of these bars had three additional strain gages each at 16, 25, and 31 in. (406, 635, and 787 mm) away from the midpoint.

Longitudinal strains in core concrete in the critical regions were measured using LVDTs at different locations along the section depth. In the stub specimens, the gage lengths varied between 2.0 and 7.0 in. (51 and 102 mm) and covered a length of 15 in. (381 mm) from the stub-column interface. In the prismatic specimen, a 4.5 in. (114 mm) gage length was used at the midsection and at an adjacent section. The deflection of each specimen along its length was also measured with LVDTs.

Testing

All the specimens were tested under cyclic lateral load to large inelastic deformations while simultaneously being subjected to constant axial loads. Fig. 4 shows the test frame with

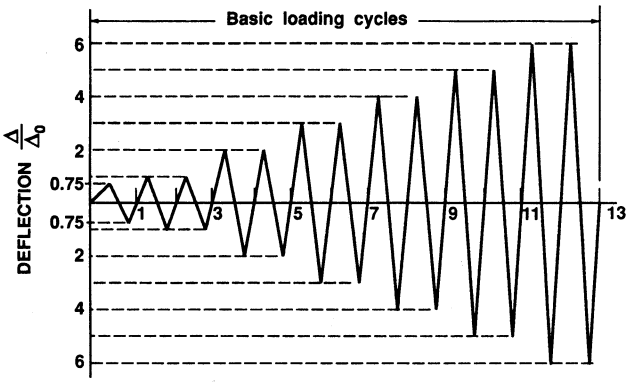

Fig. 5—Specified displacement history

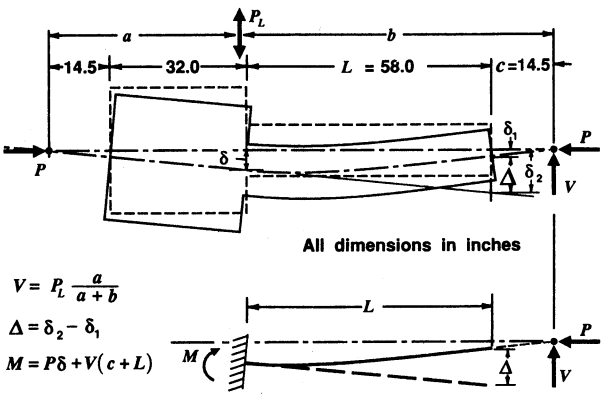

Fig. 6—Idealization of specimen

the prismatic specimen, the critical middle region of which was subjected to axial load and cyclic flexure. In the case of nonprismatic specimens, the lateral load was applied at the stub about 4 in. (102 mm) away from the stub-column interface. Thus, the most critical region of the column subjected to axial load, shear, and flexure was adjacent to the stub.

Details of the test setup and test procedure are available elsewhere.[7,10] A few necessary details are given here. As shown in Fig. 4, all the specimens were tested horizontally. At each end of a specimen, a hinge was attached that allowed the specimen to rotate freely about the axis of the shaft in the hinge. The same shaft was used to support the specimen. This mechanism allowed the line of action of the axial load to remain unchanged throughout the test. Preparations before a test included alignment of the specimen, which required application of axial load and monitoring of strain at various locations in the column.

Actual testing started with the application of full axial load followed by the application of lateral load using the displacement history shown in Fig. 5. The displacement Δ_o was calculated theoretically and may be defined as the yield or elastic lateral displacement for the unconfined concrete specimen, at which the specimen behavior departs significantly from a straight line. About 8 to 12 min were required to complete one cycle. The loading was stopped or slowed to a very low rate at selected points to permit recording data, marking cracks, and taking photographs. Three X-Y plotters were used to trace continuous plots of load versus displacements and deformations at various locations. After several cycles in the inelastic range, the tests were terminated by monotonically loading the specimen in the lateral direction to failure in the cycle in which the specimen could not maintain the axial load.

TEST RESULTS

Results are presented here primarily in the form of lateral load-versus-displacement and moment-versus-curvature relationships. Fig. 6 shows the lateral load V and displacement Δ used for nonprismatic specimens in Fig. 7 through 9. For the prismatic specimen, the lateral load applied and deflection at midspan were used in Fig. 10. In nonprismatic specimens, failure did not occur at the sections of maximum moment adjacent to the stubs. Due to the confinement provided by the stubs, failure moved away by several inches to a section carrying smaller moment. Moment and curvature values in Fig. 7 through 9 are for the most damaged sections. The theoretical moment and load capacities are also shown in Fig. 7 through 10. Moment M_i was calculated for the unconfined section using the ACI Building Code.[6] The loads V_i and P_i were determined to produce M_i at the critical section without considering P-Δ effect.

Test observations

Compared to normal strength concrete (NSC) specimens,[7] spalling of cover concrete in HSC specimens was more abrupt, extensive as well as widespread. Cracking of cover concrete started in the first load cycle at strains ranging from 0.002 to 0.0035 and during the fourth cycle cover was completely lost. In Specimens AS-3H, AS-18H, and A-17H, the maximum lateral load and moment occurred in the fourth cycle, and in Specimen AS-20H the maximum response was measured in the sixth load cycle. Specimen AS-3H lasted for five complete cyclic reversals of predetermined displacement and the failure in the sixth load cycle was triggered by the buckling of three side bars along the section depth. In Specimen AS-18H, four corner bars were observed to have buckled in the sixth load cycle but the specimen still behaved in a stable manner. In the seventh load cycle, the specimen failed following a bursting noise of an inner tie fracture at about 10.5 in. (267 mm) from the stub face. In Specimen AS-20H, four corner bars were observed to have buckled in the tenth load cycle and the specimen failed in the eleventh cycle. Behavior of Specimen A-17H was similar to that of Specimen AS-3H except that the effect of cover spalling in A-17H is more pronounced. Both specimens could undergo only one complete load cycle after the cover concrete was completely destroyed. It was noticed that the severe damage in Specimen A-17H extended beyond the instrumented region, and therefore the M-ϕ curve in Fig. 10 somewhat underestimated section deformability.

Ductility parameters

In evaluating the column performance and studying the effects of different variables, ductility and toughness were defined using parameters shown in Fig. 11. These include cur-

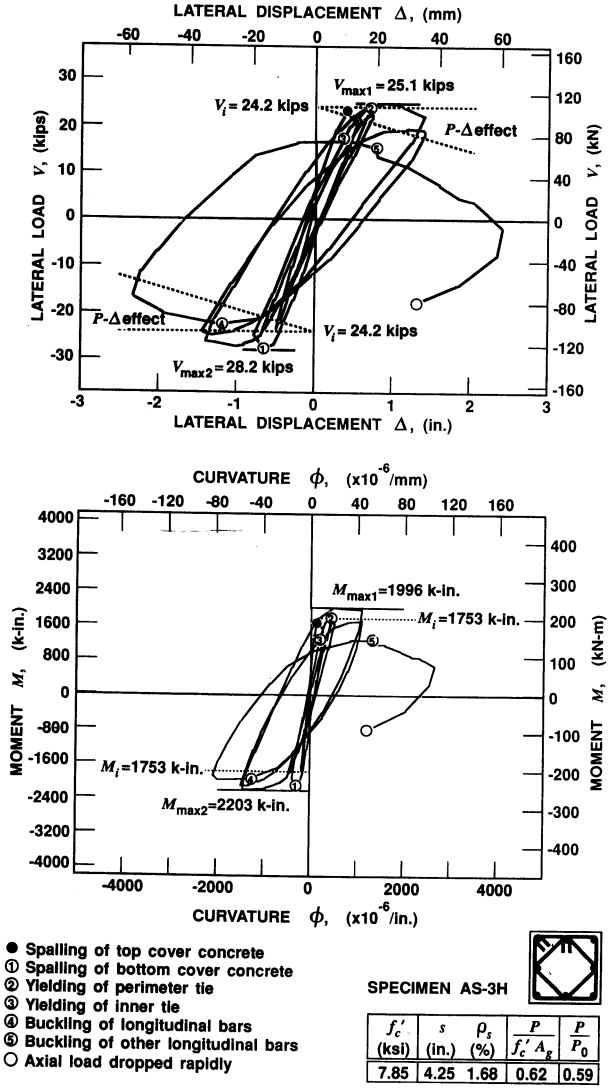

f_c' (ksi)	s (in.)	ρ_s (%)	$\frac{P}{f_c' A_g}$	$\frac{P}{P_0}$
7.85	4.25	1.68	0.62	0.59

Fig. 7—Behavior of Specimen AS-3H

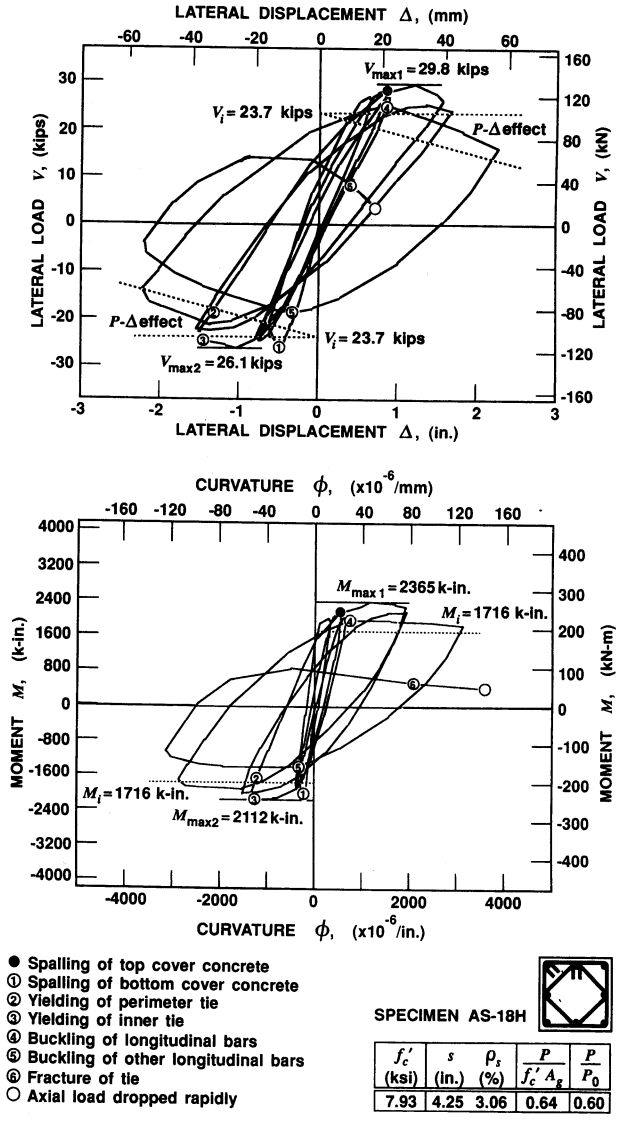

f_c' (ksi)	s (in.)	ρ_s (%)	$\frac{P}{f_c' A_g}$	$\frac{P}{P_0}$
7.93	4.25	3.06	0.64	0.60

Fig. 8—Behavior of Specimen AS-18H

vature and displacement ductility factors (μ_ϕ and μ_Δ), cumulative ductility ratios (N_ϕ and N_Δ), energy-damage indicator E, and work-damage indicator W. Subscripts t and 80 wherever used indicate, respectively, the value of the parameter until the end of the test (total value) and the value until the end of the cycle in which the force or the moment is dropped to 80 percent of the maximum value. Energy parameters e_i and w_i represent the areas enclosed in the cycle i by the M-ϕ and V-Δ loops, respectively. All other terms are defined in Fig. 11 except L_f and t, which represent the length of the most damaged region and section depth of the specimen, respectively. Whereas the ductility factors and cumulative ductility ratios represent the deformability of the section or member, the damage indicators estimate toughness. The work-damage indicator W is similar to the one proposed by Ehsani and Wight.[11] Table 1 lists the ductility parameters for all the specimens that can be directly compared. In addition to the four specimens discussed in the preceding, results from three comparable NSC specimens[7] are also included to evaluate different variables.

DISCUSSION OF RESULTS

A general observation from the results shown in Fig. 7 through 10 can be made that high-strength concrete with about 8000 psi (55.2 MPa) compressive strength can be made to behave in a fairly ductile manner under high axial loads if appropriate confinement detailing is used. It is now well known that distribution of longitudinal and lateral steel plays an important role in the mechanism of confinement.[9] The steel configuration used here was chosen based on earlier tests on NSC specimens[12] and was expected to provide effective confinement to the core. From the current series of tests and tests reported earlier,[7] the variables that can be examined for their effects on column behavior include the amount of lateral steel, concrete strength, presence of stub, and the axial load level.

Amount of lateral steel

The amount of lateral steel determines the extent of lateral pressure on core concrete. If the distribution of lateral and longitudinal steel is such that a large portion of the core area is effectively confined,[13] the confinement mechanism is very

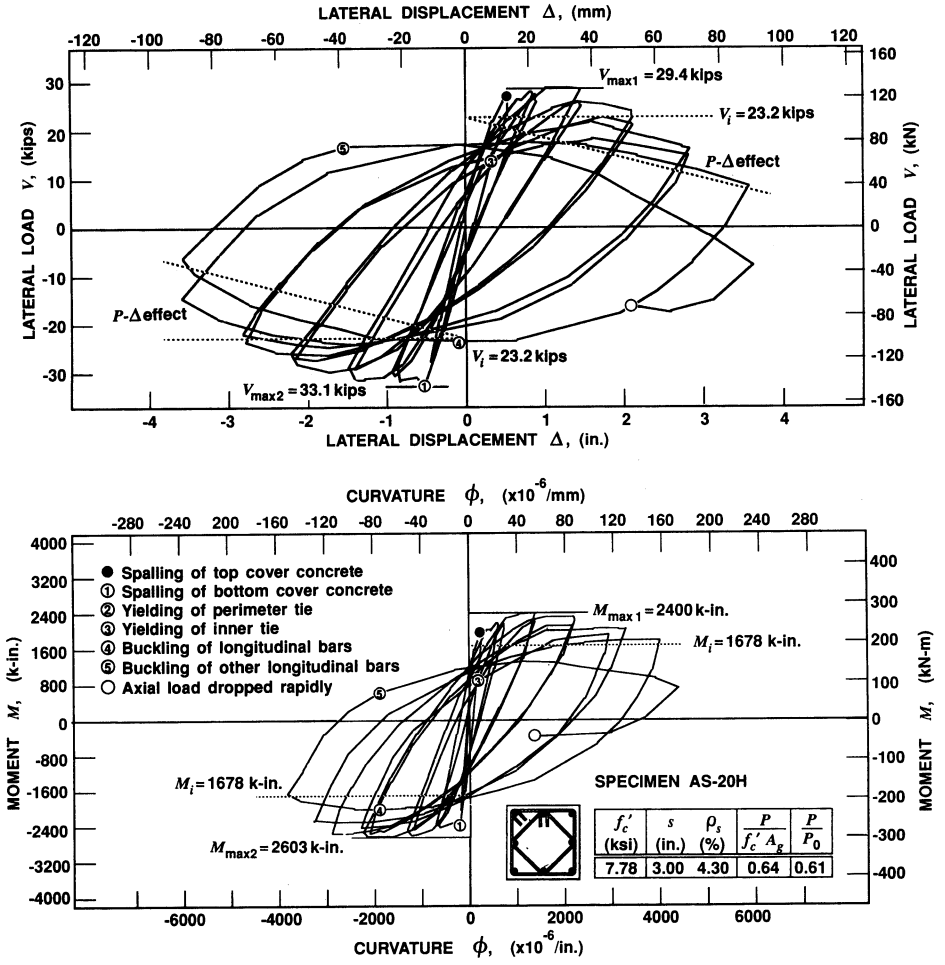

f_c' (ksi)	s (in.)	ρ_s (%)	$\frac{P}{f_c' A_g}$	$\frac{P}{P_0}$
7.78	3.00	4.30	0.64	0.61

Fig. 9—Behavior of Sepcimen AS-20H

efficient and a change in the amount of lateral steel results in a significant change in column behavior, as is obvious from a comparison of the responses of Specimens AS-3H, AS-18H, and AS-20H. All three columns were subjected to the same level of axial load and the same lateral load excursions. Whereas the only notable difference between Specimens 3H and 18H is the amount of lateral steel, the tie spacing in Specimen 20H is an additional variable compared to the other two specimens. An increase in ρ_s significantly improved column behavior. The reduction of tie spacing from 4.25 in. (108 mm) in Specimens 3H and 18H to 3.0 in. (76 mm) in Specimen 20H contributed somewhat to the improvement of column behavior, but the increase in the amount of tie steel is believed to have had the major effect. Only Specimen 20H, which contained about twice the code-required tie steel, was capable of maintaining a stable response, with μ_ϕ exceeding 15. Specimen 18H, which meets the code requirement[6] for the amount of tie steel, showed reasonably ductile behavior, but was able to resist only six load cycles, as opposed to ten for Specimen 20H. From the average of ductility parameters listed in Table 1, it appears that an increase in the lateral reinforcement ratio results in an almost proportional increase in ductility.

The axial load level used in these specimens was large and exceeded the allowable limits[6] by about 7 percent, which can happen during a severe earthquake. The results show that an appropriate amount of well-detailed tie steel can produce a ductile column even under such a high axial load. For less adverse conditions and low performance level, the design of confining steel can be adjusted accordingly.

Concrete strength

Three NSC specimens, AS-3, AS-17, and AS-18, are added to the list of specimens to evaluate the effect of concrete strength on confinement (Table 1). All these specimens were similar in shape to the HSC nonprismatic specimens and tested in the same manner. Specimens AS-3 and AS-3H contained the same amount of tie steel and were tested under the same level of axial load, as determined by $P/f_c' A_g$. Specimen AS-3H showed relatively brittle behavior compared to Specimen AS-3 (Fig. 7 and 12). It resisted only five complete load cycles compared with eleven for Specimen AS-3. All the ductility parameters (Table 1) for AS-3H are significantly smaller than those for AS-3. A similar conclusion can be drawn from a comparison of Specimens A-17H and A-3, shown in Fig. 13. Specimen A-3 was prismatic and tested in a way similar to that for Specimen A-17H, except that the lateral load was applied monotonically.[12] Slightly higher $P/f_c' A_g$ in Specimen A-17H is not believed to be entirely responsible for the difference in the responses of the two specimens.

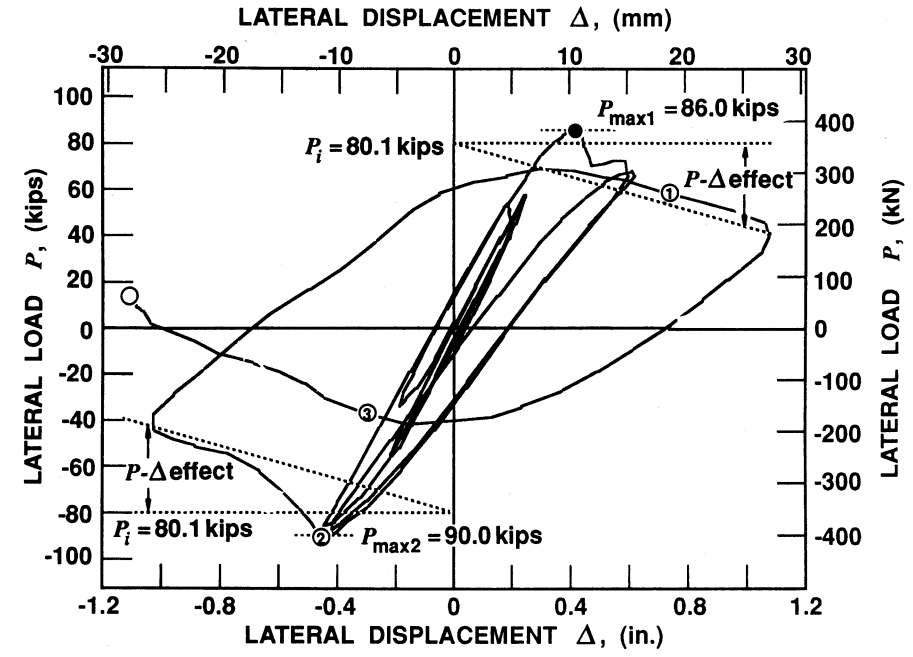

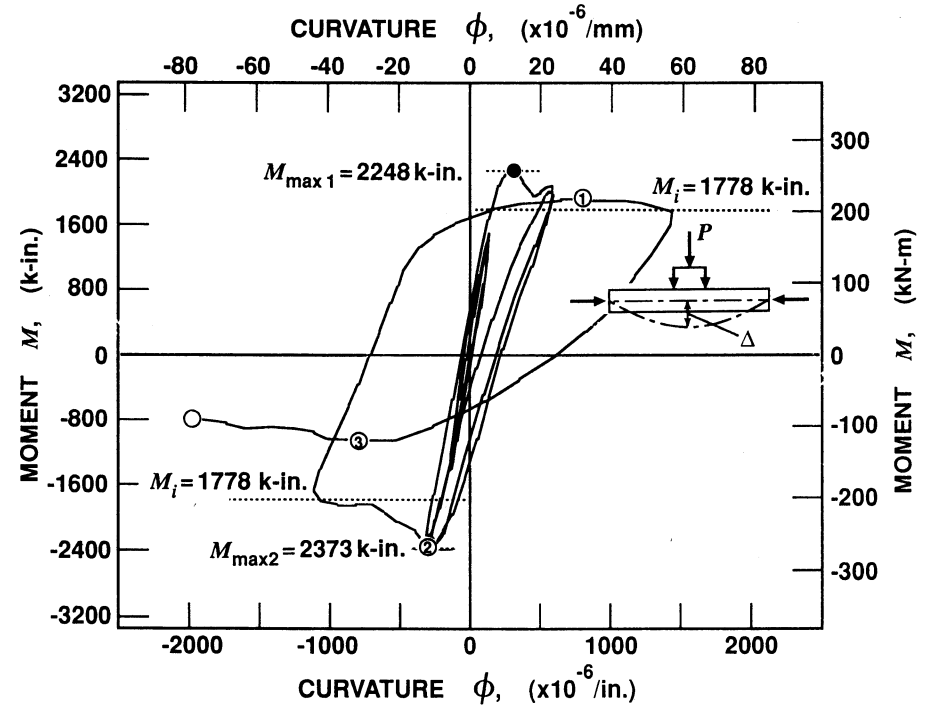

● Spalling of top cover concrete
① Buckling of top middle bar
② Spalling of bottom cover concrete
③ Buckling of 5 additional bars
○ Axial load dropped rapidly

SPECIMEN A-17H

f_c' (ksi)	s (in.)	ρ_s (%)	$\frac{P}{f_c' A_g}$	$\frac{P}{P_0}$
8.57	4.25	1.68	0.65	0.62

Fig. 10—Behavior of Sepcimen A-17H

Specimens AS-3 and AS-18H contained about 44 percent higher tie steel than that required by the ACI Building Code,[6] and both were tested under $P/f_c' A_g \approx 0.6$. A comparison of these two specimens in Fig. 8 and 12, and Table 1, shows that although the enhancement in section moment capacities due to confinement in both the specimens is very similar, the ductility and energy-absorption capacity of the HSC specimen is considerably lower. The axial load on Specimen AS-3 was about 11 percent below the allowable limit[6] however, for Specimen AS-18H, applied axial load exceeded the limit by about 8 percent. Fig. 14 shows results from Specimen AS-17, which is comparable to Specimen AS-18H from the point of view that both contained approximately 150 percent of the code-required tie steel and were tested under axial loads that were approximately 60 percent of the ultimate axial load-carrying capacity P_o. Load-deflection and moment-curvature responses, and the ductility parameters (Table 1) of these two specimens, are reasonably similar. A second pair of specimens (AS-18 and AS-20H) can also be studied for the same variable from Fig. 9 and 15. A comparison of the performance of the failed sections in five relevant specimens is shown in Fig. 16, where the moment as a fraction of the maximum value reached during each test is plotted against the cumulative curvature ductility ratio and energy-damage indicator. Considering small differences in the amount and spacing of tie steel, the responses of comparable specimens of different concrete strengths tested under similar level of axial load P/P_o are very similar. "Comparable specimens" means that the steel distributions in the specimens are similar and the amount of lateral steel is proportional to the concrete strength, i.e., the ratios between the amount of tie steel used and the amount required by the code[6] are almost equal in the specimens.

It appears that the required amount of tie steel for a given performance of a column under a certain axial load measured as a fraction of P_o is proportional to concrete strength f_c'. However, this increased amount of tie steel for higher strength concrete is not needed to compensate for the loss of strength due to cover spalling but to maintain the integrity of the core to provide ductile behavior. Detailing of steel therefore becomes important.

Stub effect

Specimens AS-3H and A-17H had critical sections reinforced, detailed, and loaded in a similar manner except that the section in the prismatic specimen was not subjected to shear from the lateral load. The main difference, however, between the two specimens was the location of the critical section, which in Specimen AS-3H was adjacent to a heavy stub and did not fail. The failure moved away to the adjacent critical section due to the restraint provided by the heavy undamaged stub. A comparison of the moment-curvature behavior of the failed sections of the two specimens (Fig. 7 and 10) shows only a slight difference between the two specimens. Higher strength of Specimen A-17H can be attributed to the higher concrete strength, and slightly less ductile behavior of this specimen can be explained by the fact that the most severe damage took place outside the instrumented region, as mentioned earlier. Although not directly comparable, the load-displacement responses of the two specimens indicate a similarity of behavior. The sections where failure initiated in the stub specimens appear to be mostly free of the stub restraint. Fig. 17 shows the photographs of the failed sections of the three nonprismatic specimens at the end of the tests, along with sketches of the specimens indicating the most damaged regions. The moments M_{smax} at the critical sections of the columns adjacent to the stubs were about 6 to 8 percent higher than those M_{max} at the critical sections (Table 1). The higher moments did not cause failure at the critical sections and therefore the extent of flexural strength enhancement due to stub restraint is unknown. The center of the most damaged zone is approximately 8 to 9 in. (203 to 229 mm) from the stub. In the capacity design approach for earthquake resistance, appropriate corrections should be made in the calculation of design shear in columns where the critical sections are adjacent to the heavy elements such as beam-column joints. If the actual flexural capacity of the section is unknown, the shear force should be based on the moment capacities of the plastic hinges and the distance between them, which is approximately h to $2h$ less than the column length where h is the column depth.

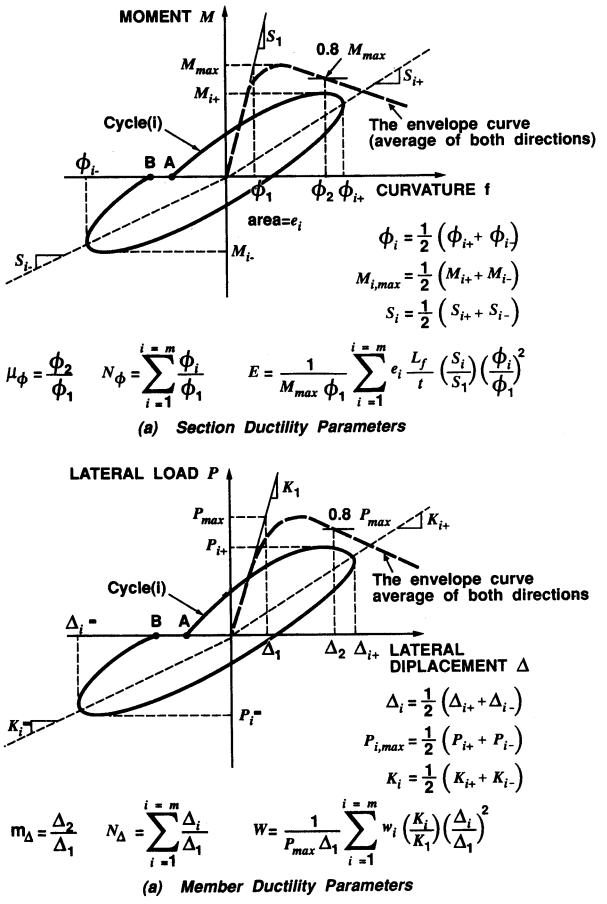

Fig. 11—Definitions of ductility parameters

Concrete deformability

Measured maximum compressive strain values in concrete corresponding to various events are listed in Table 2 for high-strength concrete stub specimens. The strains at first visible cracking are in the extreme fiber of cover concrete. For other

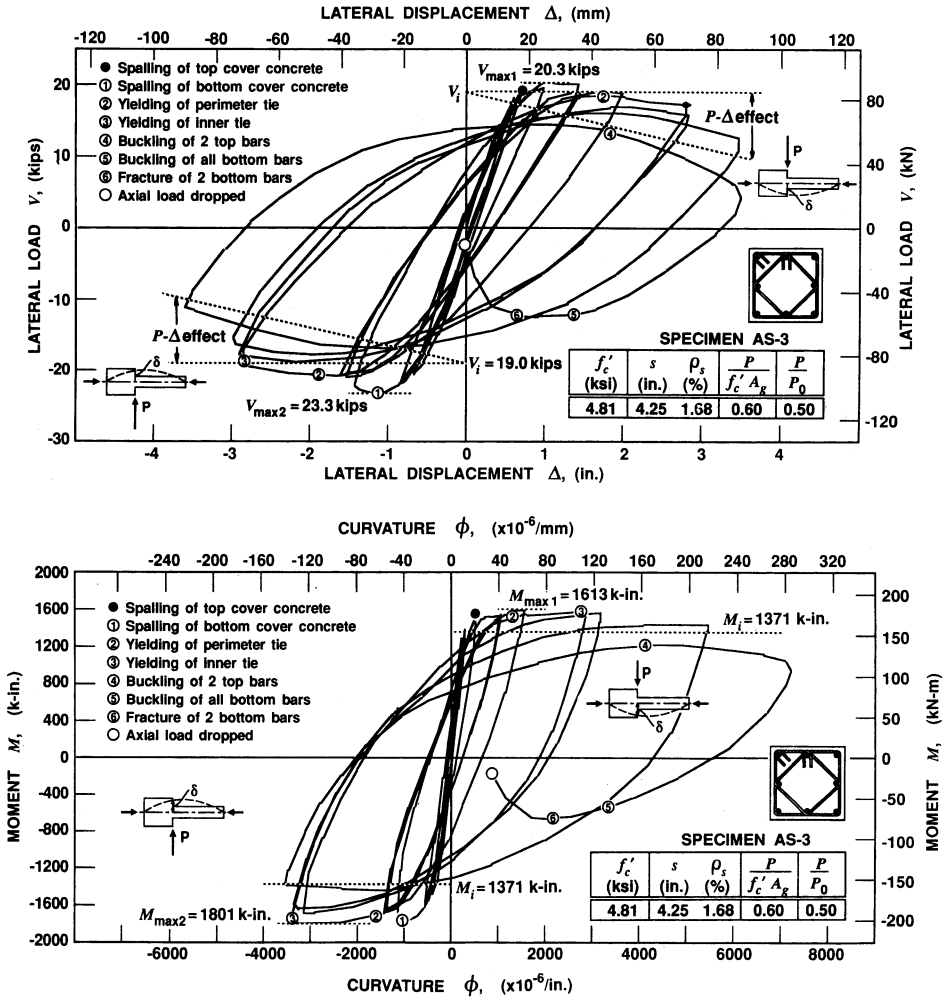

Fig. 12—Behavior of Specimen AS-3

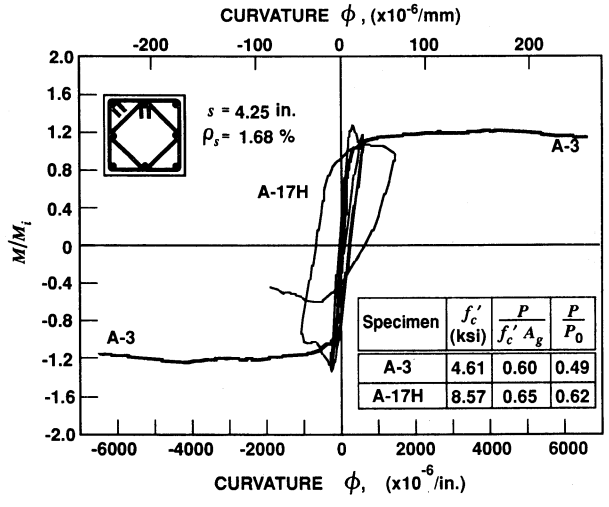

Fig. 13—Effect of concrete strength

events, the strain values refer to the extreme fibers in the core. These values are averaged for loading in both directions. Failure strain is the maximum strain measured during the last complete load cycle. Strain corresponding to 80 percent of the maximum moment beyond peak can be considered as the useful or useable strain and, with appropriate confinement, can be as large as 0.02 for HSC [$f_c' \approx 8000$ psi (55.2 MPa)] columns. Comparable strains for NSC columns were approximately in the range of 0.03.

Equivalent plastic hinge length

Assuming that most of the inelastic rotation takes place in the plastic hinge over which the plastic curvature is constant, the hinge length L_p can be calculated for a cantilever from the following equation

$$\Delta_p = \Delta_{max} - \Delta_1 = (\phi_{max} - \phi_1) L_p L'$$

where Δ_1 and ϕ_1 are as defined in Fig. 11 and L' = length from column end to the center of the plastic hinge. The plastic hinge length was calculated for each load cycle in which μ_Δ was 4 or larger. In any event, L_p was calculated for at least the last two load cycles. The average L_p for each of the three nonprismatic specimens is given in Table 2, and is approximately equal to a section size of 12 in. (305 mm). The same observation was made for six similar NSC specimens[7] in which L_p varied between $0.85h$ and $1.1h$ with an average value of $1.02h$. It appears that the plastic hinge length is independent of variables such as steel configuration, axial load level, amount of confining steel, and concrete strength.

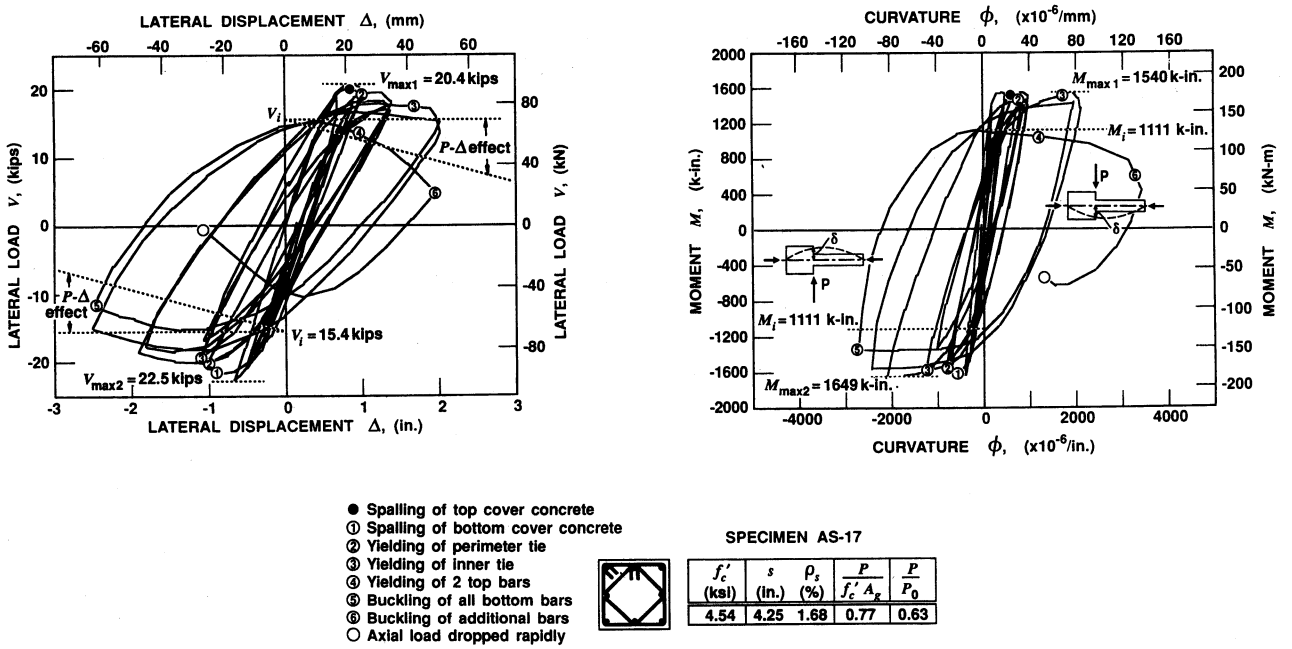

f_c' (ksi)	s (in.)	ρ_s (%)	$\frac{P}{f_c' A_g}$	$\frac{P}{P_0}$
4.54	4.25	1.68	0.77	0.63

Fig. 14—Behavior of Specimen AS-17

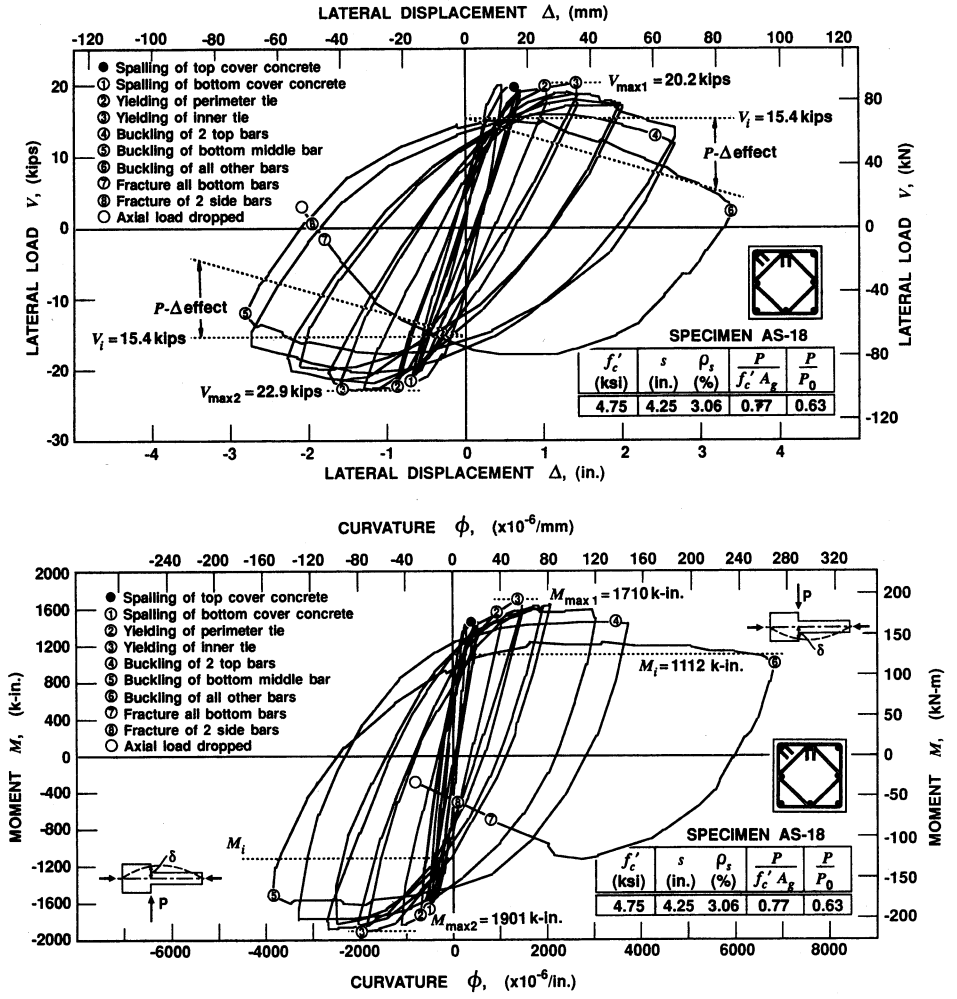

f_c' (ksi)	s (in.)	ρ_s (%)	$\frac{P}{f_c' A_g}$	$\frac{P}{P_0}$
4.75	4.25	3.06	0.77	0.63

Fig. 15—Behavior of Sepcimen AS-18

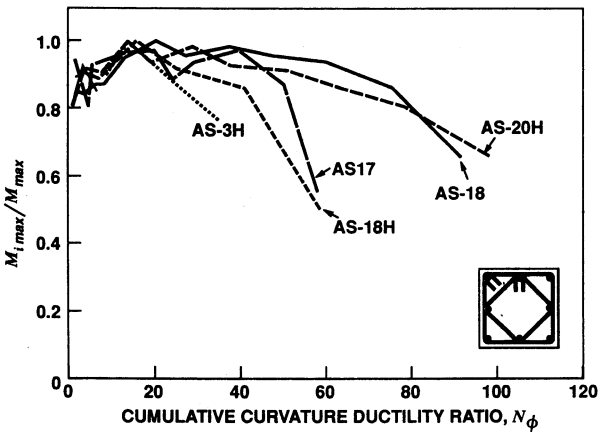

(a) Moment-Curvature Ductility Ratio Curves

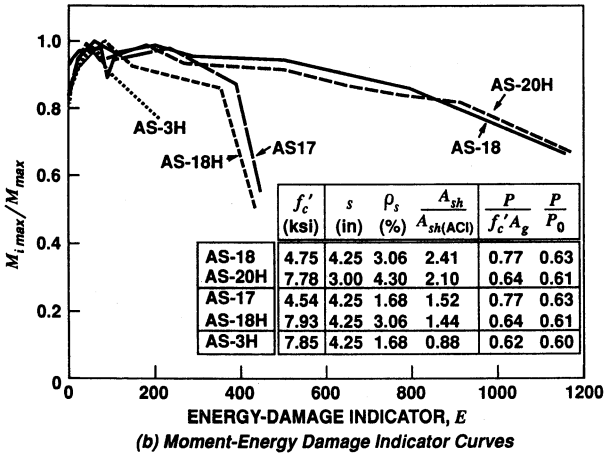

	f_c' (ksi)	s (in)	ρ_s (%)	$\frac{A_{sh}}{A_{sh(ACI)}}$	$\frac{P}{f_c' A_g}$	$\frac{P}{P_0}$
AS-18	4.75	4.25	3.06	2.41	0.77	0.63
AS-20H	7.78	3.00	4.30	2.10	0.64	0.61
AS-17	4.54	4.25	1.68	1.52	0.77	0.63
AS-18H	7.93	4.25	3.06	1.44	0.64	0.61
AS-3H	7.85	4.25	1.68	0.88	0.62	0.60

(b) Moment-Energy Damage Indicator Curves

Fig. 16—Comparison of ductility parameters for specimens with varied concrete strength

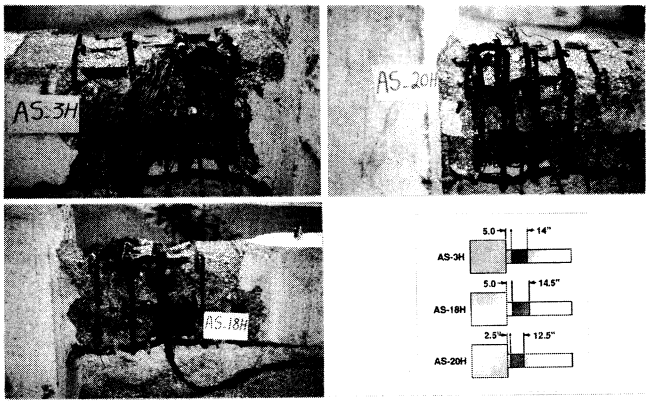

Fig. 17—Specimens at end of tests and sketches of most damaged regions

Table 2 — Concrete strain and plastic hinge length

Specimen	Concrete compressive strain at: First visible cracking	M_{max}	0.8 M_{max}	Failure*	Equivalent plastic hinge length: L_p, in.	L_p/h
AS-3H	0.0019	0.005	0.013	0.023	12.7	1.05
AS-18H	0.0021	0.020	0.021	0.025	10.7	0.89
AS-20H	0.0035	0.010	0.021	0.050	13.0	1.08

*Corresponding to maximum applied displacement in the last complete cycle as an average of both load directions.

SUMMARY AND CONCLUSIONS

Four column specimens made of high-strength concrete with nominal strength of 8000 psi (55.2 MPa) were tested under constant axial load and cyclic lateral load. Results were compared with those from earlier similar specimens of normal strength concrete. The following conclusions can be drawn from this study.

As in NSC specimens, the amount of lateral steel has a significant effect on the response of HSC specimens. Improvement in ductility and energy-absorption capacity appears to be proportional to the increase in lateral steel content, while the effect on the section moment capacity is less than proportional. Ultimate compressive strains in the range of 0.01 to 0.02 and curvature ductility factors as high as 16 were observed in the 8000 psi (55.2 MPa) concrete confined by rectilinear ties, and subjected to large axial load, cyclic flexure, and shear.

For the same amount of tie steel, the flexural ductility of HSC columns was significantly less than that of comparable NSC specimens tested under similar $P/f_c' A_g$ values. For the same percentage of the confining steel required by the ACI Building Code, NSC columns displayed better ductility than comparable HSC columns tested under similar $P/f_c' A_g$. However, for the same level of axial load measured as a fraction of P_o (the ultimate axial load capacity), HSC and NSC columns behaved similarly in terms of energy-absorption characteristics when the amount of tie steel in the columns was in proportion to the unconfined concrete strength. Conversely, the amount of confining steel required for a certain column performance appears to be proportional to the concrete strength as long as the applied axial load is measured in terms of P_o rather than $P/f_c' A_g$. The heavy stub provides additional confinement to the adjacent section and causes the failure to move to another section where the stub-restraining effect is minimal. In HSC specimens, the maximum moments at the failed sections varied between 120 and 150 percent of the theoretical capacities without confinement. Moments at the stub-column interfaces that were 6 to 7 percent higher than that at the failed sections did not cause failure there. In the absence of the actual capacity of the critical sections, design shear for the columns in the capacity design approach should be based on the hinges' moment capacities and the length between the plastic hinges, which may be h to $2h$ smaller than the clear column length where h is the section depth.

Confining steel designed according to North American building codes can provide satisfactory column behavior for a certain situation. For other situations, such as varied steel detailing, axial load level, different performance requirements, etc., the design may be either unnecessarily conservative or unsafe.

ACKNOWLEDGMENTS

Research reported here was supported by grants from the Texas Advanced Research Program and the Natural Sciences and Engineering Research Council of Canada, and is gratefully acknowledged.

REFERENCES

1. "High Strength Concrete, State-of-the-Art Report," *FIP/CEB Bulletin d'Information* No. 197, FIP-London, Aug. 1990, 61 pp.

2. Uzumeri, S. M., and Basset, R., "Behavior of High Strength Concrete Members," *Proceeding of the Symposium on Utilization of High Strength Concrete,* Stavangr, Norway, June 1987, pp. 237-248.

3. Nilson, Arthur H., "High-Strength Concrete—An Overview of Cornell Research," *Proceeding of the Symposium on Utilization of High Strength Concrete,* Stavangr, Norway, June 1987, pp. 27-38.

4. Leslie, K. E.; Rajagopalan, K. S.; and Everard, N. J., "Flexural Behavior of High Strength Concrete Beams," ACI JOURNAL, *Proceedings* V. 73, No. 9, Sept. 1979, pp. 517-521.

5. Muguruma, H., and Watanabe, F., "Ductility Improvement of High-Strength Concrete Columns with Lateral Confinement," *Utilization of High Strength Concrete—Second International Symposium,* SP-121, American Concrete Institute, Detroit, 1990, pp. 47-60.

6. ACI Committee 318, "Building Code Requirements for Reinforced Concrete and Commentary (ACI 318-89/ACI 318R-89)," American Concrete Institute, Detroit, 1989, 353 pp.

7. Khoury, S. S., and Sheikh, S. A., "Behavior of Normal and High Strength Confined Concrete Columns with and without Stubs," *Research Report* No. UHCEE 91-4, Department of Civil and Environmental Engineering, University of Houston, Dec. 1991, 338 pp.

8. Saatcioglu, M., "Deformability of Reinforced Concrete Columns," *Earthquake-Resistant Structures—Inelastic Response and Design,* SP-127, American Concrete Institute, Detroit, 1991, pp. 421-452.

9. Sheikh, S. A., and Uzumeri, S. M., "Strength and Ductility of Tied Concrete Columns," *Journal of the Structural Division,* ASCE, V. 106, ST 5, May 1980, pp. 1079-1102.

10. Shah, D. S., and Sheikh, S. A., "Behavior of High Strength Concrete Columns under Axial Load and Cyclic Flexure, *Research Report* No. UHCEE 91-5, Department of Civil and Environmental Engineering, University of Houston, Dec. 1991, 182 pp.

11. Ehsani, M. R., and Wight, J. K., "Confinement Steel Requirements for Connections in Ductile Frames," *Journal of the Structural Division,* ASCE, V. 116, St 3, Mar. 1990, pp. 751-767.

12. Sheikh, S. A., and Yeh, C. C., "Tied Concrete Columns under Axial Load and Flexure," *Journal of the Structural Division,* ASCE, V. 116, No. 10, Oct. 1990, pp. 2780-2801.

13. Sheikh, S. A., and Uzumeri, S. M., "Analytical Model for Concrete Confinement in Tied Columns," *Journal of the Structural Division,* ASCE, V. 108, ST 12, Dec. 1982, pp. 2703-2722.